Monodisperse iron oxide nanoparticles by thermal decomposition – elucidating particle formation by second-resolved *in situ* small-angle X-ray scattering

A. Lassenberger[†§], T. A. Grünewald[‡§¤], P.D.J. van Oostrum[†], H. Rennhofer[‡], H. Amenitsch[⊥], R. Zirbs[†], H.C. Lichtenegger[‡]* and E. Reimhult[†]*

[†] Department of Nanobiotechnology, Institute for Biologically Inspired Materials, University of Natural Resources and Life Sciences, Muthgasse 11, 1190 Vienna, Austria.

[‡] Department of Material Science and Process Engineering, Institute of Physics and Materials Science, University of Natural Resources and Life Sciences Peter-Jordan Strasse 82, 1190 Vienna, Austria

[⊥]Institute for Inorganic Chemistry, Graz University of Technology, Stremayrgasse 9/V, 8010 Graz, Austria

[§] equally contributing

Table S1. Extracted numerical parameters from all reactions

Core size	**Heating rate [K/min]**	**Burst nucleation (Porod) peak / °C**		**Burst nucleation (Porod) peak / min after 290°C**		**Onset of growth**		**Plateau length (Invariant)**	**Radius / nm**		**Final PD**	
		Start of peak	peak maximum	Start of peak	Peak maximum	°C	time after 290°C / min		@60 min	Final	@60 min	lowest
L	1	276	284	-		279		220 °C - 276 °C	3.92	3.9	0.4	0.57
L	3	-	-	0.8	6.1	-	0.5	240 °C - 0.75 min	4.4	4.5	0.5	0.4
L	9	-		5.9	10.9	-	2.6-9.1	235 °C - 5.5 min	4.3	4.4	0.7	0.6
M	3	255	259	-		~260	-	247 °C - 255 °C	2.2	2.2	0.8	0.7
S	3	240-250		-		240-250	-	--	1.3	1.3	1.7	
S	9	245	249	-		245	-	--	1.56 nm		0.85	0.9

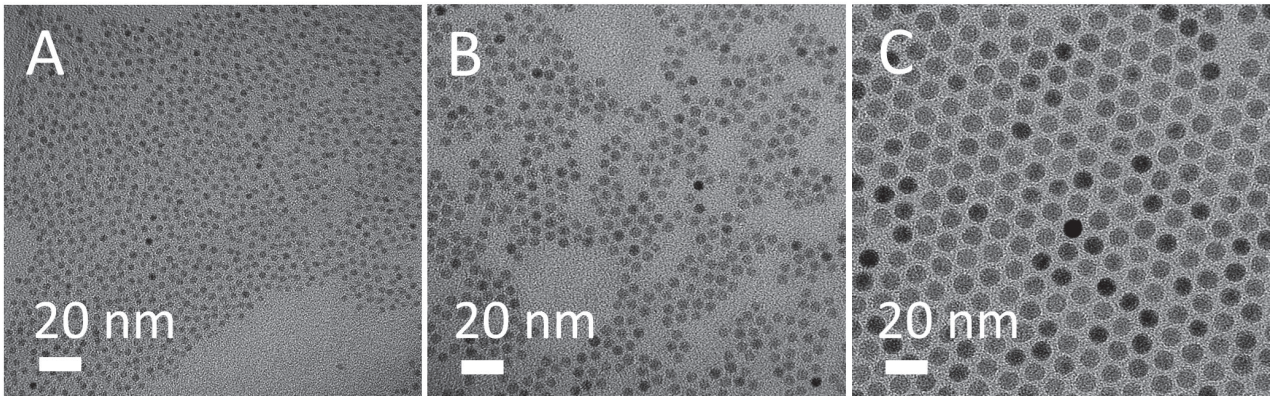

Figure S1. Transmission electron micrographs of final NP sizes of A) 'Small', B) 'Medium' and C) 'Large' NPs.

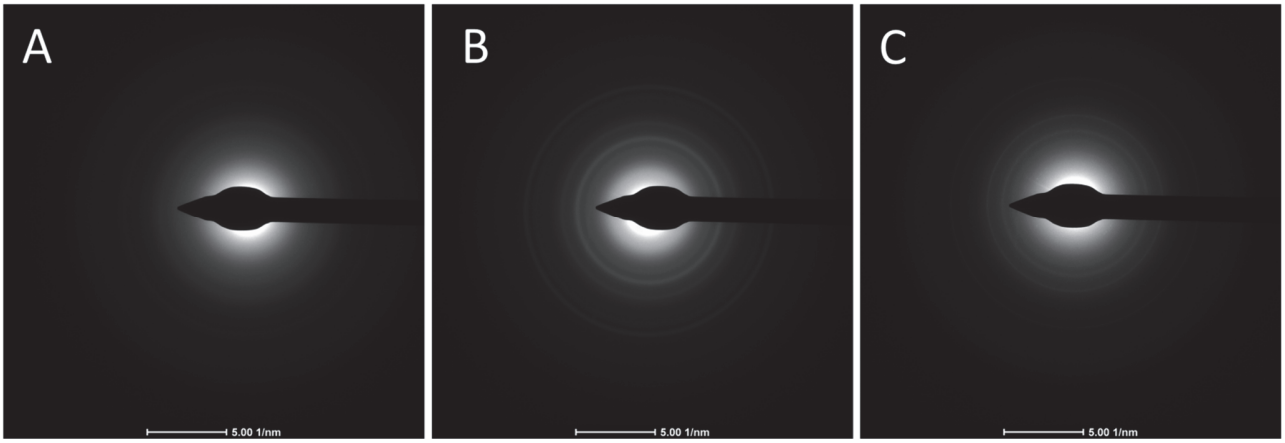

Figure S2. Electron diffraction patterns of final NP sizes of A) 'Small', B) 'Medium' and C) 'Large' NPs showing that the NPs are crystalline

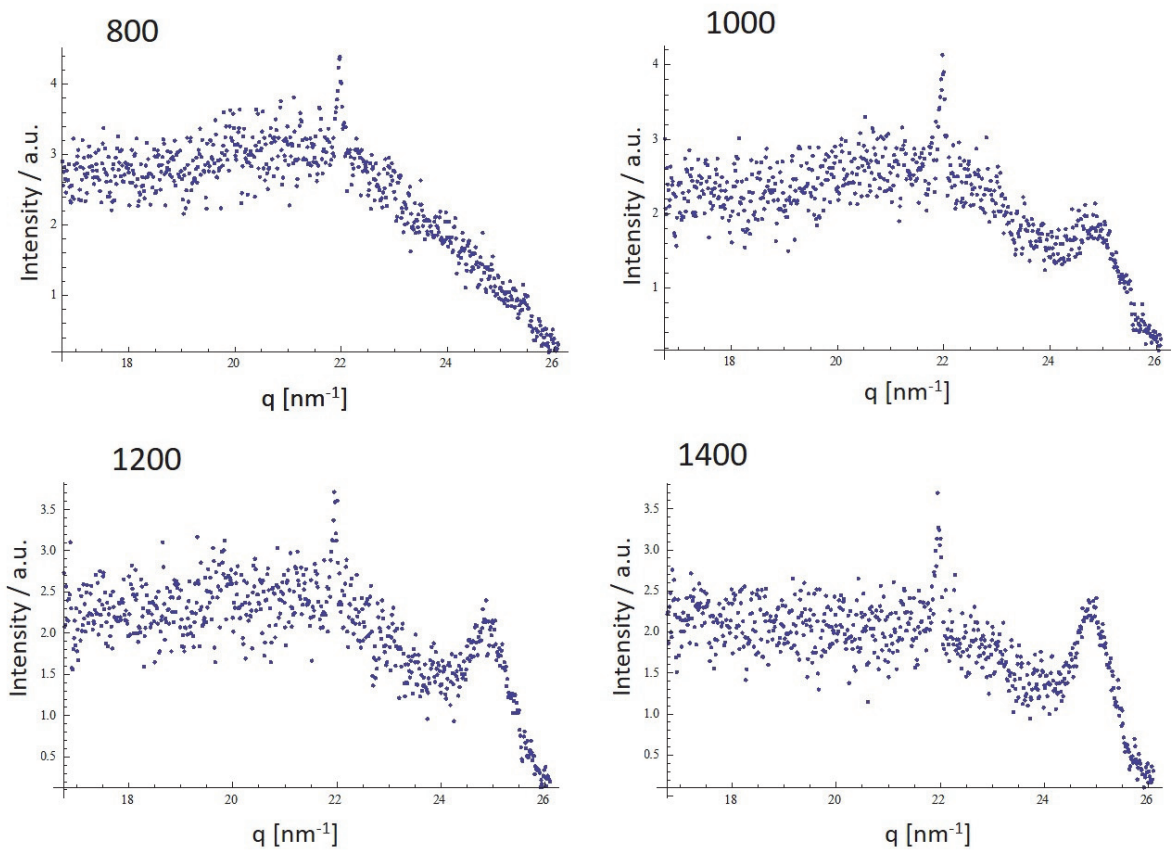

Figure S3. WAXS patterns from the synthesis of 'Large' NPs at different data points. Data point 800 marks the onset of crystallinity, data points 1000, 1200 and 1400 are taken at roughly the same time as the electron diffraction patterns shown in Figure 3 of the main text. WAXS patterns clearly show the increasing crystallinity throughout the synthesis.

DETAILED EXPERIMENTAL DESCRIPTION

DIFFERENT PUMPING SCHEME

In order to assess the possibility of beam-induced nucleation and general beam damage effects, an intermittent pumping scheme was used with the aim of replacing the volume in the measurement cell as fast as possible and illuminating the same portion for two minutes continuously (0.5 s exposure time every 10 s). A heating rate of 3 K/min and large particles were synthesized during this run. A total of 29 pumping and measurement cycles was carried out.

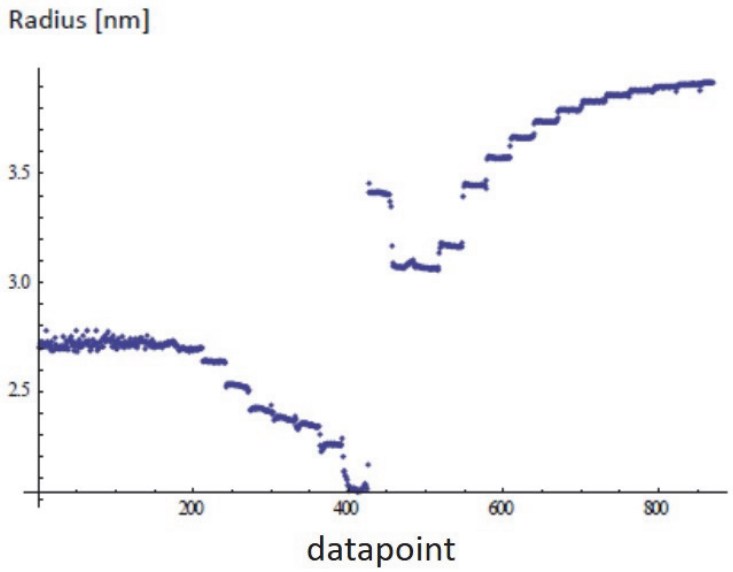

Figure S4. Evolution of the radius during the intermittent pumping scheme.

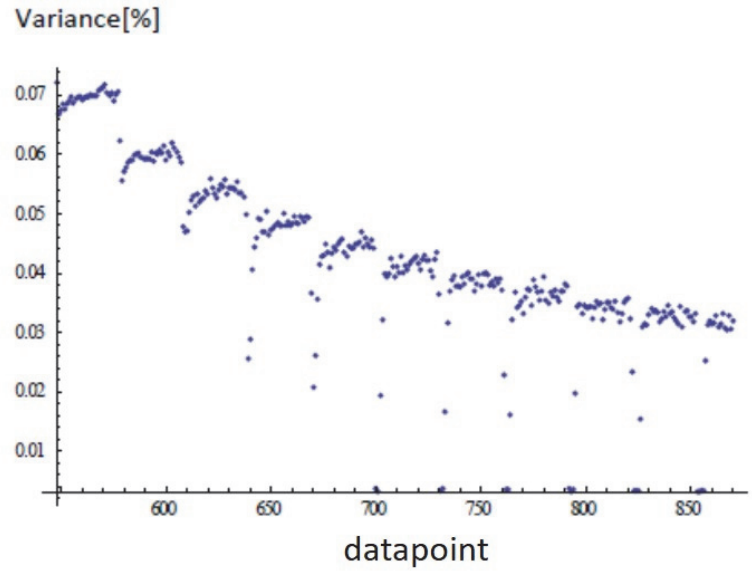

Figure S5. Evolution of the polydispersity during the intermittent pumping scheme.

Neither the radius (Figure S4) nor the polydispersity (Figure S5) show sign of beam damage. The end and beginning of each intermittent measurement are smeared due to the pumping action.

EXPERIMENTAL SETUP

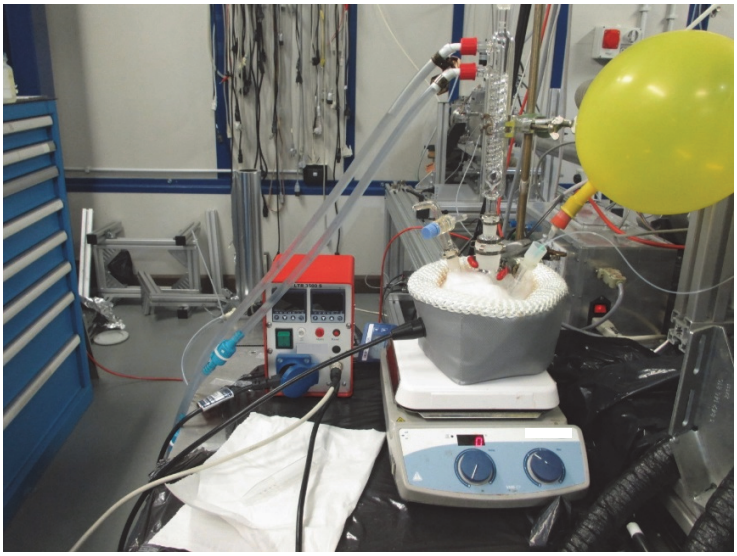

Figure S6. Reflux setup for the NP synthesis.

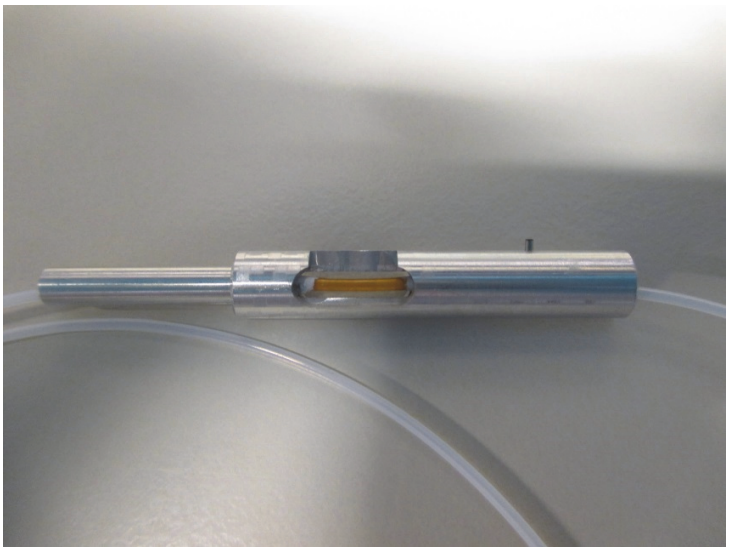

Figure S7. Measurement cell with a Kapton window.

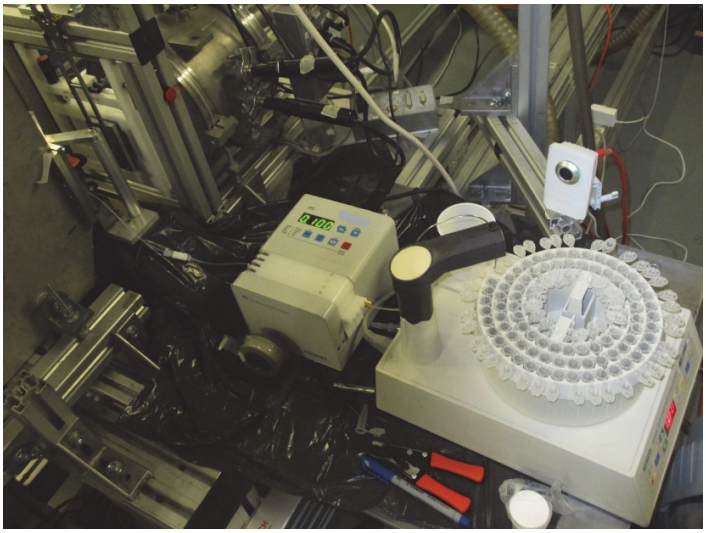

Figure S8. Sample pumping and outlet collection

Figures S5, S6 and S7 show pictures of the critical parts of the experimental setup. The reaction vessel (Figure S5) was connected to the measurement position having a Kapton tubing window (Figure S6) by ~70 cm of tygon tubing. Due to the strong temperature dependence of all reactions the reaction was immediately quenched upon entry of the sample into the tubing. The measurement cell composed of Kapton tubing was changed for each experiment to prevent contamination. The complete pumping system (Figure S7) was calibrated prior to each run and at this instance also the reproducibility of the previous setting was tested but no significant deviations were detected.

FLUX NORMALIZATION

To match the temperature in the reaction vessel with the SAXS/WAXS signal and the fractions of the autosampler the time lag between the extraction of a sample and the measurement at the X-ray window was taken into account.

The volume of a droplet V_{Drop} was calculated as follows:

$$V_{Drop} = \frac{Flux}{N_{Drop}} \qquad \text{Equation 1}$$

where Flux is the flow rate at the beginning of the experiment and N_{Drop} the number of drops per time increment. This volume can be used to convert the droplet count at the outlet into a flow curve over the course of the experiment.

The nominal temperature $T_{nom}(i)$ for each SAXS/WAXS frame *i* was calculated as:

$$T_{nom}(i) = T_{Start} + \frac{i \cdot rate}{\frac{1}{frlen}} \qquad \text{Equation 2}$$

where T_{Start} is the temperature in the reaction vessel at the start of the experiment, rate the heating rate and *frlen* the frame length of a SAXS/WAXS frame. This does not take the temperature offset between the different components into account, hence based on the tube volume V_{off} between the reaction vessel and the respective component, the offset can be calculated as

$$offset = \frac{V_{off}}{flux} \qquad \text{Equation 3}$$

which can be subtracted from T_{nom} to obtain the matched temperature that used for further comparison.